

Left atrial appendage occlusion simulation based on three-dimensional printing: new insights into outcome and technique



Vlad Ciobotaru^{1*}, MD; Nicolas Combes², MD; Claire A. Martin^{3,4}, MD, PhD; Eloi Marijon⁵, MD; Eric Maupas¹, MD; Augustin Bortone¹, MD; Eric Bruguière², MD; Jean-Benoit Thambo³, MD, PhD; Emmanuel Teiger⁶, MD, PhD; Pénélope Pujadas-Berthault¹, MD; Julien Ternacle⁶, MD; Xavier Iriart³, MD

1. Hôpital Privé «Les Franciscaines», Nîmes, France; 2. Pediatric and Adult Congenital Heart Disease Department, Clinique Pasteur, Toulouse, France; 3. CHU Bordeaux, Bordeaux, France; 4. Papworth Hospital NHS Trust, Cambridge, United Kingdom; 5. Hospital Georges Pompidou, HEGP, Paris, France; 6. CHU Henri Mondor, Créteil, France

This paper also includes supplementary data published online at: http://www.pcronline.com/eurointervention/135th_issue/29

KEYWORDS

- LAA closure
- non-invasive imaging
- specific closure device/technique

Abstract

Aims: The aim of this study was to assess the predictive value of simulation based on 3D-printed models before left atrial appendage occlusion (LAAO) for peri-device leaks (PDL) and the impact on procedural outcomes compared to conventional imaging.

Methods and results: Seventy-six patients referred for LAAO with double disc device underwent construction of a 3D-printed LA model using flexible photopolymer resin. An implant simulation was performed retrospectively in Group 1 (55 patients), blinded to implanted device size, and prospectively in Group 2 (21 patients). In Group 1, an off-axis device position occurred in 14 patients (25%) and the incidence of PDL was 27% (15 patients); mismatch between model and device size was the best predictor (area under the curve 0.88, CI: 0.77-0.99). When using 3D simulation prospectively, mean prosthesis number per patient (1.05±0.21 vs. 1.20±0.52, p=0.04) and incidence of leaks (5% vs. 27%, p<0.01) were reduced compared to conventional imaging alone, as well as fluoroscopy time (19 mins [13.4-23] vs. 13.5 mins [11.1-15], p=0.012) and total fluoroscopy dose (7,291 [1,811-12,734] vs. 1,978 (1,548-4,800) mGy·cm², p=0.029).

Conclusions: 3D-printed patient-specific adaptive and flexible LA models improve LAAO double disc device sizing. This can potentially reduce procedure time and the number of prostheses employed per patient.

*Corresponding author: Hôpital Privé Les Franciscaines, 3 Rue Jean Bouin, 30000 Nîmes, France.
E-mail: vcobotaru@yahoo.fr

Abbreviations

AF	atrial fibrillation
AUC	area under the curve
IAS	interatrial septum
LA	left atrium
LAA	left atrial appendage
LAAO	left atrial appendage occlusion
LZ	landing zone
MDCT	multidetector computed tomography
NPV	negative predictive value
OS	ostium
PDL	peri-device leak
PPV	positive predictive value
ROC	receiver operating characteristic
TEE	transoesophageal echocardiography

Introduction

Percutaneous left atrial appendage occlusion (LAAO) has emerged as an alternative approach to long-term oral anticoagulation in the prevention of atrial fibrillation (AF) mediated stroke, in high-risk patients with contraindications to long-term oral anticoagulation¹. Two devices are currently available in Europe: the WATCHMAN® (Boston Scientific, Marlborough, MA, USA) and AMPLATZER™ Amulet™ (St. Jude Medical [now Abbott], St. Paul, MN, USA), an evolution of the AMPLATZER™ Cardiac Plug (ACP) (St. Jude Medical). Recent registries with both devices have demonstrated high procedural success and low complication rates^{2,3}. However, to achieve this, a full understanding of LAA anatomy and optimal device selection are critical.

Manufacturers' sizing recommendations for double disc St. Jude devices are currently based solely on measurement of the maximal diameter of the landing zone (LZ). However, as this alone may not be sufficient to guarantee complete disc coverage of the LAA ostium (OS), additional anatomic information is mandatory, including appendage shape, ostium eccentricity, LZ depth and morphology of the left superior pulmonary venous ridge. Despite the use of multimodality imaging⁴, optimal sizing and device positioning remain challenging in some cases^{5,6}, possibly due to the limitation of current imaging modalities to evaluate LAA anatomy and its relationship with surrounding structures perfectly. This has led to an alternative approach using three-dimensional (3D)-printed models to integrate all anatomical factors influencing device sealing.

Objectives

We aimed to assess the additional value of 3D-printed modeling of the LAA, compared to traditional multimodality imaging alone, in the setting of double disc device implantation for predicting peri-device leaks or device malposition. We hypothesised that a systematic approach including preoperative simulation of device implantation using a 3D-printed model of the LAA and surrounding structures may be helpful to improve LAAO procedure outcomes.

Methods

Of 133 patients referred for LAAO in three French institutions between 2015 and 2017, 76 with preprocedural and post-procedural cardiac computed tomography (CT) were included in the study. Fifty-two (52) patients did not have complete imaging, and a further three patients were excluded due to inadequate imaging quality. The follow-up was 17±10 months.

Two consecutive cohorts were analysed.

1. In the first group of 55 patients we retrospectively evaluated the additional value of 3D-printed models in predicting device sizing and risk of peri-device leaks (defined as a gap of >5 mm between the occluder disc and the LAA wall). A simulation was performed on the 3D-printed model after the procedure, blinded to implanted device size during LAAO.
2. In the second group of the subsequent 21 consecutive patients, we prospectively explored the additional clinical value of a 3D-printed model simulation in addition to multimodality imaging, in terms of LAAO efficacy, fluoroscopy time and number of prostheses used per patient. Two patients were excluded due to contraindication to contrast agents.

Intravenous contrast-enhanced multidetector CT (MDCT) (**Figure 1**) was performed in all patients prior to and post LAAO as well as per-procedural 3D transoesophageal echocardiography (TEE) (**Figure 2**). Cavity segmentation was performed on CT DICOM data automatically, and subsequently manually adjusted to include the entire LA. 3D printing was performed on a stereolithographic 3D printer (Form 2 plus; Formlabs, Somerville, MA, USA) using flexible photopolymer resin (additional methodological data and **Supplementary Figure 1** included in the **Supplementary Appendix**).

Written informed consent was obtained from all patients. The study protocol was approved by the hospitals' institutional ethics committees.

STATISTICAL ANALYSIS

Baseline characteristics were expressed by descriptive statistics. Normal continuous variables were summarised as mean±standard deviation. Non-normally distributed variables were compared using Mann-Whitney U tests and presented as median and interquartile range. Categorical variables were compared using Fisher's exact test.

Receiver operating characteristic (ROC) curve analysis was performed for 3D-printed sizing and imaging modality (CT or TEE) sizing. Stepwise logistic regression was used to assess for univariate and multivariate predictors for peri-device leaks and off-axis position. The statistical software used was XLSTAT, version 10.12.06 (Addinsoft, Paris, France).

Results

DEMOGRAPHIC, CLINICAL AND PROCEDURAL DATA

Amulet devices were implanted in 67 patients and ACP devices in nine patients. Procedural success was 98%, with one unsuccessful procedure due to inadequate sheath alignment. Mean age was 78±7 years and 29 patients (38%) were female. The mean

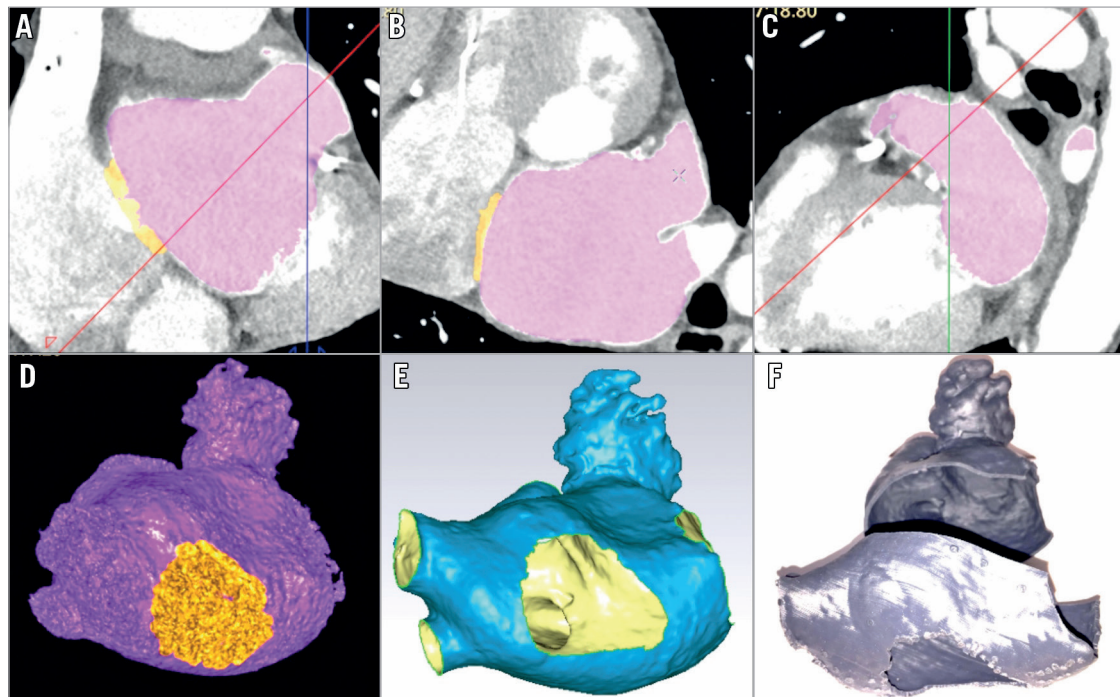


Figure 1. Views of the LAA from CT imaging and 3D-printed models. A)-C) Multiplanar CT view of left atrium (LA) showing orthogonal views of segmented CT with LA in violet, with the thin interatrial septum (IAS) in orange. D) Volume-rendered CT images of the LA (violet) and thin IAS (orange). E) Standard tessellation language (STL) file format of the entire LA, including LAA, thin IAS (central hole), pulmonary veins and ridge (inside face coloured in yellow, outside in blue). F) LA 3D-printed model obtained from STL data (two interlocking parts showing separation between left and right pulmonary veins).

CHA₂DS₂-VASc score was 4.9±1.1 and the HAS-BLED score was 4.1±0.8, with a history of cerebral haemorrhage in 39 (52%) patients and digestive haemorrhage in 21 (28%). A prior history of stroke or transient ischaemic attack was present in 25 (34%) patients, impaired renal function (renal clearance <50 ml/min) in 29 (39%), and congestive heart failure in 22 (29%). Forty-four (44; 58%) were discharged post procedure on dual antiplatelet therapy (DAPT), 23 (30%) on aspirin alone, and nine (12%) on low molecular weight heparin or vitamin K antagonists (VKA).

CT max LZ diameter was 22.6±4.9 mm and TEE diameter 20.2±5 mm. Eccentricity index, defined as the ratio of minimal diameter to maximal diameter, was 0.85±0.1. Inter-observer variability for the CT measurement of the mean LZ diameter was 0.17±2.9 mm.

USE OF 3D-PRINTED MODELS IN DEVICE SIZING

An incomplete LAA occlusion with a gap (**Figure 3**) between the disc and OS wall of >5 mm was observed in 15 of 55 patients (27%) in Group 1. All patients with a gap showed residual LAA opacification. A mismatch between the predicted size from the 3D-printed model and the device size actually used (**Figure 4**) was the best predictor of peri-device leaks (AUC 0.88, CI: 0.77-0.99) with positive predictive value (PPV) of 77% and negative predictive value (NPV) of 95%. In comparison, conventional sizing had significantly lower predictive values (AUC=0.53 and 0.60, respectively,

for CT and TEE, p<0.001) (**Table 1**). In logistic regression, mismatch with sizing determined by the 3D-printed model was the highest predictive factor for peri-device leak (**Table 2**).

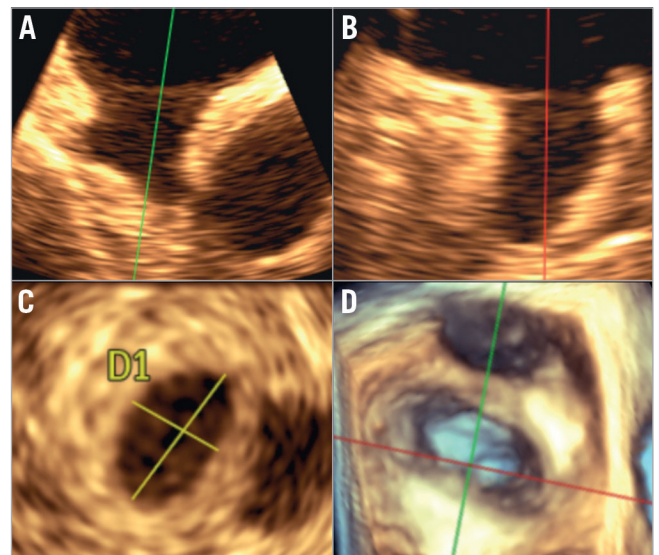


Figure 2. TEE method of landing zone measurements. Measurements of the landing zone are performed 10 mm distal to the ostium in two orthogonal planes (A & B) and a third transverse plane (C). D) 3D-TEE view of LAA.

Table 1. Receiver operating characteristic (ROC) curve analysis for Group 1 for 3D-printed, CT and TEE sizing, with post-LAO peri-device leakage as the outcome measure.

Variable	AUC	p-value	Se	Sp	PPV	NPV
3D-printed sizing	0.88 (0.77-0.99)	–	87%	90%	77%	95%
CT sizing	0.53 (0.38-0.69)	<0.001	47%	60%	30%	75%
TEE sizing	0.60 (0.46-0.74)	<0.001	33%	87%	50%	78%
TEE+CT sizing	0.60 (0.43-0.77)	<0.001	60%	55%	33%	79%

p-value compares ROC curve analysis for a specific variable versus that for 3D-printed sizing. AUC: area under the curve; NPV: negative predictive value; PPV: positive predictive value; Se: sensitivity; Sp: specificity

Table 2. Predictors of peri-device leakage and off-axis position.

Variable	Predictors of peri-device leak				Predictors of off-axis position			
	Univariate		Multivariate		Univariate		Multivariate	
	OR (95% CI)	p-value	OR (95% CI)	p-value	OR (95% CI)	p-value	OR (95% CI)	p-value
3D-printed sizing mismatch	30.2 (8.2-111.1)	<0.01	33.3 (7.8-117.2)	<0.01	3.1 (1.1-9.5)	0.07	–	–
CT sizing mismatch	1.8 (0.65-5.0)	0.29	–	–	–	–	–	–
TEE sizing mismatch	1.7 (0.6-5.0)	0.31	–	–	–	–	–	–
LZ eccentricity	2.3 (0.8-6.2)	0.06	–	–	–	–	–	–
Inadequate transseptal puncture site	1.15 (1.01-1.31)	0.12	–	–	35.1 (10.2-120.1)	<0.01	36.2 (9.8-124.3)	<0.01
“Chicken wing” morphology	1.6 (0.6-4.4)	0.43	–	–	–	–	–	–
Large ridge	1.3 (0.5-3.6)	0.61	–	–	6.8 (2.1-23.1)	<0.01	7.3 (1.8-24.7)	<0.01

LZ eccentricity is the ratio of minimum:maximum LZ diameter. Significant p-values are in bold. LZ: landing zone; OR: odds ratio in univariate analysis

Overall, periprocedural device exchange occurred in nine patients (16.3%) using 11 extra devices, with exchange for a larger prosthesis in four patients and a smaller one in five patients. The

number of devices used was 1.2 per patient. Consequently, if information from 3D-printed models had been applied, a different prosthesis size may have been used in 17 patients (31%), with nine receiving a smaller prosthesis and eight a larger one.

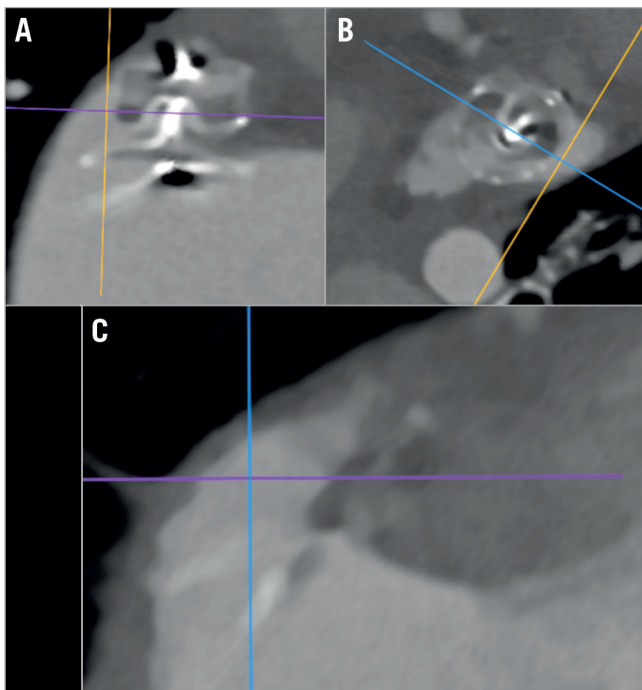


Figure 3. Multi-oblique CT view post LAO. Note the large peri-device gap (A & B) with a residual LAA cavity (C) (same case as in Figure 4A).

USE OF 3D-PRINTED MODELS IN TRANSEPTAL PUNCTURE ORIENTATION

Figure 5 shows transseptal delivery sheath positioning at the interatrial septum (IAS) and resultant device position in preprocedural and periprocedural imaging, and modelled by 3D-printed simulation. An off-axis device position was observed in Group 1 in 14 patients (25%), independently of the correspondence between the CT device sizing and the device used (AUC=0.49). The highest predictive factors for an off-axis device position were a large pulmonary ridge and suboptimal transseptal puncture location (Table 2). Using 3D-printed models, the misalignment would have been corrected using a different transseptal puncture site in 18 patients (33%).

Manufacturer guidelines suggest that a transseptal puncture should be performed in the postero-inferior quadrant, which was the initially intended puncture site for all patients in the prospective Group 2 based on imaging alone. However, in 10 patients (47%) in Group 2, use of the 3D model simulation suggested that the optimal puncture should be in a different quadrant, with an antero-inferior quadrant in five patients and median-inferior in five. Thus, off-axis positioning was significantly reduced (p<0.01), with only one patient demonstrating an off-axis device position due to non-concordance between the 3D-printed model-oriented transseptal site and the one eventually used.

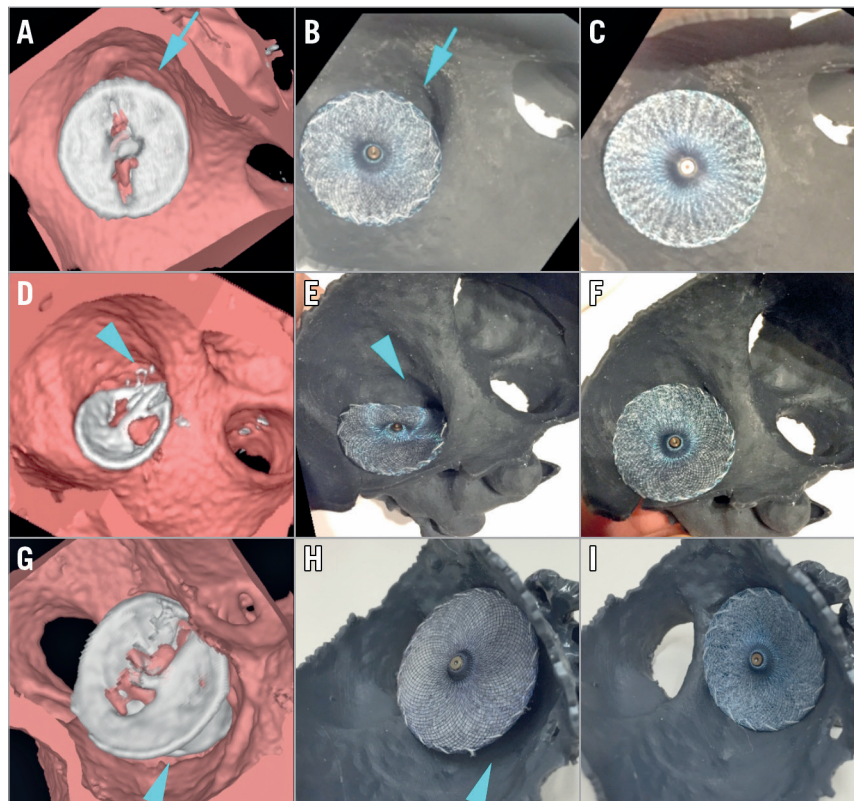


Figure 4. 3D view of volume-rendered CT scans and corresponding 3D-printed model images. 3D view of volume-rendered CT scans with device in situ (A, D, G) and 3D-printed simulation using the same device (B, E, H) and one of optimal size (C, F, I). A) CT showing a large gap between the Amulet with 18 mm disc and the LAA ostium (blue arrow), as predicted by the 3D-printed model (blue arrow) with the same device (B). Simulation suggests the Amulet 20 mm disc would be the optimal choice, with complete coverage of the LAA ostium (C). D) CT showing off-axis positioning with significant residual LAA cavity (blue arrow) and a large pulmonary ridge, reproduced by a corresponding printed model simulation (E) and adequate sealing with a one size larger device (F). G) CT showing prosthesis malposition, with protrusion of the lobe (blue arrow). This is reproduced with an identical device simulated by a printed model (H). An optimal seal can be achieved using a device one size smaller (I).

CLINICAL IMPACT OF GUIDANCE FROM 3D MODELS

Among the 21 patients in Group 2 who underwent LAAO guided additionally by 3D-printed models, the mean number of prostheses used was 1.05±0.21 per patient, with only one change of prosthesis required, compared to 1.20±0.52 with conventional imaging alone (p=0.04). The incidence of leaks was significantly reduced in Group 2 compared to Group 1 (5% vs. 27%, p<0.01), with only one case demonstrating a periprocedural device leak. Use of 3D-printed models in addition to imaging modalities led to a pre-procedural change of decision concerning device sizing in eight of 21 patients; three patients required a larger device than the CT predicted, whereas five patients required a smaller one.

Fluoroscopy time (19 mins [13.4-23] vs. 13.5 mins [11.1-15], p<0.01) and total fluoroscopy dose were both significantly reduced by using 3D-printed model guidance compared to in those in whom it was not used (Table 3).

PROCEDURAL OR PERIPROCEDURAL COMPLICATIONS

In Group 1, three non-haemodynamically significant pericardial effusions and two tamponades occurred. Three patients with

Table 3. Clinical impact of 3D-printed sizing.

	Group 1 Conventional imaging N=55	Group 2 Conventional imaging+3D printed model N=21	p-value
Peri-device leaks	15 (27%)	1 (5%)	0.006
Off-axis	14 (25%)	1 (5%)	0.010
Devices per procedure	1.20	1.05	0.047
Failed implantation	1	0	NS
Fluoroscopy dose (mGy·cm ²)	7,291 (1,811-12,734)	1,978 (1,548-4,800)	0.029
Fluoroscopy time (min)	19 (13.4-23)	13.5 (11.1-15)	0.012
Sizing changed by 3D-printed model*	17 (31%)	8 (38%)	0.75
Puncture site oriented alternatively to postero-inferior as per 3D-printed model	18 (33%)	10 (47%)	0.35

Data presented as median (interquartile range). *Clinical decision would have changed in Group 1 if 3D model sizing had been applied.

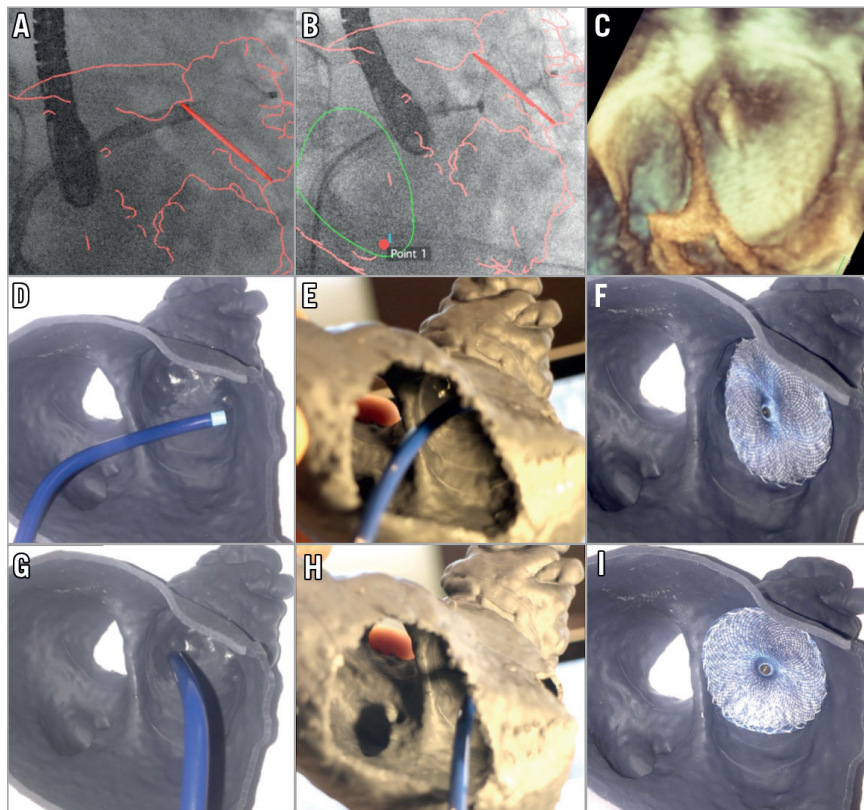


Figure 5. Impact of transseptal puncture location on sheath-LAA alignment. A)-C) Right anterior oblique fluoroscopic projection with CT fusion of the LA: suboptimal transseptal TorqVue™ (St. Jude Medical) delivery sheath orientation through the thin LAS (outlined in green) leads to misalignment with respect to the LZ plane (red) (A & B). The optimal transseptal puncture location is shown (point 1). C) 3D-TEE image of the resultant off-axis device. D)-F) 3D-printed model simulation showing misalignment of the sheath in an en face view (D) and in a view through the LAS (E), and with a resultant off-axis device. G)-I) 3D-printed model simulation showing adequate alignment of the sheath with transseptal puncture in an inferior-anterior position in an en face view (G) and in a view through the LAS (H), corresponding to red point 1 in panel B. This orientation results in adequate device sealing (I) in the simulation.

off-axis prostheses developed silent delayed device-related thrombus, detected on follow-up cardiac CT that obliged the re-initiation of anticoagulant treatment with thrombus resolution at six-month follow-up. There was no renal deterioration following CT. Adapted protocols were applied in order to use a minimum contrast volume of about 50 ml. Two Group 1 patients developed renal failure post LAAO; they had long procedure times, and significant haemoglobin drops. There were no complications in Group 2.

Discussion

DEMOGRAPHIC, CLINICAL AND PROCEDURAL DATA

In France, LAAO may only be performed in patients with a minimum CHA₂DS₂-VASc score ≥ 4 and thus our population has higher comorbidities compared to that included in prior registry data for LAAO procedures. This may explain the higher procedural complication rate in Group 1 compared to recent registry data³.

3D-PRINTED MODELLING AND OUTCOMES

We used an anatomical definition of leakage according to the Saw description, i.e., a gap >5 mm between the occluder disc

and the LAA wall that can be assessed only by CT⁷. This critical difference from the use of echo Doppler in the WATCHMAN trial⁵ may account for discrepancies in the rate of peri-device leakage reported between previous studies using either an anatomical definition based on 3D CT or an echo Doppler definition of leakage⁸.

Manufacturer sizing charts are based only on LZ and not OS diameters; however, measurement may vary depending on the level at which it is performed, accounting for the large inter-observer variability we observed in our study. Thus, for a given OS dimension, the LZ may be narrower or larger depending on how conical the LAA is. Consequently, selecting device size on LZ diameter alone does not guarantee complete OS occlusion in all situations.

The device exchange rate and the rate of leaks were dramatically reduced in our study through the use of 3D-printed simulation, while sizing decision was modified preprocedurally in eight of 21 cases (38%). A retrospective sub-analysis of the PROTECT AF study⁵ did not demonstrate increased risk of thromboembolism with residual leak. However, the authors emphasise that this finding should be interpreted with caution due to the very low event

rate. In patients with leaks larger than 5 mm, warfarin was continued. In two registries of St. Jude devices analysed retrospectively, there was no evidence of interaction in efficacy and safety endpoints^{6,9}. However, the follow-up was limited and the incidence of neurological events was too low to derive conclusions. In the absence of larger-scale prospective clinical trials, the clinical risk of malpositioning remains unresolved¹⁰.

Transseptal puncture site and guiding sheath orientation are procedural factors that influence how the disc will seal the ostium. We observed a significant number of oblique devices in Group 1, independently of adequate sizing. Oblique device implantation creates a cul-de-sac between the disc and the ridge and that may result in incomplete LAA occlusion. In the case of a protuberant ridge, the delivery sheath may protrude out in an inappropriate oblique plane leading to inadequate positioning or difficulty catheterising the LAA at all. This may require either a second transseptal puncture or further manipulation and excessive torque movement of the guided sheath.

The manufacturer's recommended puncture site is in the postero-inferior quadrant. However, depending on LAA position, atrial volume and the pulmonary ridge prominence, an antero-inferior puncture may be more appropriate. This is explored for the first time in our 3D-printed model simulation, whereas previous studies have focused solely on printed models of the LAA¹¹ and not the entire atrium. All cases of misalignment were corrected in Group 2 by choosing an alternative puncture site to the postero-inferior one. This was based not on CT or TEE, but solely on the 3D simulation. Indeed, it is very difficult to extrapolate the optimal transseptal puncture site from the 3D CT data set because there is no available tool to simulate the exact sheath shape and to perform alignment in a double oblique plane.

A previous study of the use of 3D-printed models has shown an improvement in sizing with WATCHMAN devices implanted in 22 patients¹². The predicted device size based on simulated implantation in the 3D model matched the final implanted device in 95% (21/22) of patients, whereas TEE would have undersized the device in 45% (10/22) of patients. The CT-based size decision was congruent with the final device in 77% (17/22) of patients with four cases of oversizing and one of undersizing. In a retrospective cohort of 29 patients including 17 St. Jude devices, Goitein et al found a good correlation between 3D models based on CT and the clinically used device¹³. Our data support the findings of these previous studies in the setting of double disc devices. However, our study is the largest using 3D-printed model simulation and explores other potential advantages, such as transseptal puncture planning, which has not been previously analysed. We assess the high predictive value for leaks of 3D-printed models and, critically, examine the clinical impact of the addition of 3D-printed simulation to conventional imaging sizing.

COMPARISON WITH TEE

TEE has an important role for measuring diameters and depths at set angles according to the recommendations of the product

manufacturers. The performance of 3D-TEE has been found to be more accurate than 2D-TEE for the assessment of LAA orifice size¹⁴. In our study, all patients had a 3D-TEE examination during LAAO. Compared to other imaging modalities, CT has been shown to provide the largest LAA measurements¹⁵. Therefore, even though TEE is the conventional tool recommended by the product manufacturers on which to base device size selection, operators need to recognise the limitations of this technology in assessing the "true maximal dimensions" of the LAA and to achieve adequate volume loading prior to obtaining measurements¹⁶. Furthermore, deployment of the device is dependent not only on LAA dimensions but also on the surrounding structures, including the pulmonary ridge, OS, depth and curvature of the LAA wall, that are poorly described by TEE.

In summary, the present study emphasises an integrated approach based on both imaging and 3D printing, which assures a patient-specific, anatomically tailored approach. While the value of a complementary approach such as image fusion¹⁷ has been addressed in previous studies, our approach is simple, cost-effective and adaptable to any centre performing LAAO procedures. Finally, this method aids communication between all the participating key players involved in an LAAO procedure, including the patient.

Limitations

The principal limitation of this observational multicentre study is the relatively small population cohort. The study included only double disc LAAO devices. The method employs a comparison of two sequential cohorts, without and with the use of 3D-printed models as an aid for planning LAAO, and thus a learning curve bias may have occurred. However, the rate of actual decision change through the use of 3D-printed models in Group 2 was similar to the rate of potential decision change if 3D-printed models were to have been applied in Group 1. This demonstrates a consistent and persistent impact on procedure decisions of the 3D-printed simulation.

A further technical limitation is that the printed models require the use of a dedicated CT protocol focused on image quality optimisation to minimise artefact. Segmentation and separation between contrast blood and tissue is based on enhanced intensity voxel and is largely performed automatically but needs an experienced operator for final manual adjustment, taking into account LA and LAA anatomy. Although CT segmentation takes around 10-15 minutes, this time can potentially be saved in reduced procedure duration.

Stereolithographic material was chosen because it is simple to use, and low in cost compared with other technologies. However, despite using material with elasticity, there is a limit to the extent to which the 3D-printed model can mimic the mechanical properties of the LAA^{18,19}. 3D printing adds costs of approximately US \$200. Currently, CT scans are not always performed before LAAO in some centres, and whether a CT scan is needed for all patients or only in a specific fraction needs to be evaluated; a further study is currently underway to address cost-effectiveness²⁰.

Conclusions

Device sizing based solely on LAA neck diameter to avoid leaks and malposition has limited value. 3D-printed patient-specific adaptive and flexible LA models improve LAAO double disc device sizing, by incorporating all anatomical variations. In addition, the use of models permits critical preprocedural planning of the optimal transseptal puncture site. This can potentially lead to improved patient outcomes by reducing procedure time and the number of prostheses employed per patient.

Impact on daily practice

Percutaneous LAAO is a prophylactic technique undertaken in frail patients with high CHA₂DS₂-VASC and HAS-BLED scores with contraindications to long-term anticoagulation. Procedural success critically depends on good understanding of LAA anatomy and adequate preprocedural planning. 3D printing assures a patient-specific, anatomically tailored approach by incorporating all anatomical variations. The use of model simulation permits improved choice of device size, optimal transseptal puncture site and adequate sheath orientation, and improves patient outcomes by reducing procedure time and the number of prostheses employed per patient. This method may be integrated in a training programme, particularly in low-volume or new centres, to improve success rates.

Funding

This work was supported by “Les Franciscaines” Hospital, Nîmes, France, a member of the clinical research support structure Santé Cité-SCERI, France.

Conflict of interest statement

The authors have no conflicts of interest to declare.

References

- Reddy VY, Doshi SK, Sievert H, Buchbinder M, Neuzil P, Huber K, Halperin JL, Holmes D; PROTECT AF Investigators. Percutaneous left atrial appendage closure for stroke prophylaxis in patients with atrial fibrillation: 2.3-Year Follow-up of the PROTECT AF (Watchman Left Atrial Appendage System for Embolic Protection in Patients with Atrial Fibrillation) Trial. *Circulation*. 2013;127:720-9.
- Santoro G, Meucci F, Stolicova M, Rezzaghi M, Mori F, Palmieri C, Paradossi U, Pastormerlo LE, Rosso G, Berti S. Percutaneous left atrial appendage occlusion in patients with non-valvular atrial fibrillation: implantation and up to four years follow-up of the AMPLATZER Cardiac Plug. *EuroIntervention*. 2016;11:1188-94.
- Landmesser U, Schmidt B, Nielsen-Kudsk JE, Lam SCC, Park JW, Tarantini G, Cruz-Gonzalez I, Geist V, Della Bella P, Colombo A, Zeus T, Omran H, Piorkowski C, Lund J, Tondo C, Hildick-Smith D. Left atrial appendage occlusion with the AMPLATZER Amulet device: periprocedural and early clinical/echocardiographic data from a global prospective observational study. *EuroIntervention*. 2017;13:867-76.
- Prakash R, Saw J. Imaging for percutaneous left atrial appendage closure. *Catheter Cardiovasc Interv*. 2016 Nov 3. [Epub ahead of print].
- Viles-Gonzalez JF, Kar S, Douglas P, Dukkipati S, Feldman T, Horton R, Holmes D, Reddy VY. The clinical impact of incomplete left atrial appendage closure with the Watchman Device in patients with atrial fibrillation: a PROTECT AF (Percutaneous Closure of the Left Atrial Appendage Versus Warfarin Therapy for Prevention of Stroke in Patients With Atrial Fibrillation) substudy. *J Am Coll Cardiol*. 2012;59:923-9.
- Wolfrum M, Attinger-Toller A, Shakir S, Gloekler S, Seifert B, Moschovitis A, Khattab A, Maisano F, Meier B, Nietlispach F. Percutaneous left atrial appendage occlusion: Effect of device positioning on outcome. *Catheter Cardiovasc Interv*. 2016;88:656-64.
- Saw J, Fahmy P, DeJong P, Lempereur M, Spencer R, Tsang M, Gin K, Jue J, Mayo J, McLaughlin P, Nicolaou S. Cardiac CT angiography for device surveillance after endovascular left atrial appendage closure. *Eur Heart J Cardiovasc Imaging*. 2015;16:1198-206.
- Jaguszewski M, Manes C, Puippe G, Salzberg S, Müller M, Falk V, Lüscher T, Luft A, Alkadhi H, Landmesser U. Cardiac CT and echocardiographic evaluation of peri-device flow after percutaneous left atrial appendage closure using the AMPLATZER cardiac plug device. *Catheter Cardiovasc Interv*. 2015;85:306-12.
- Saw J, Tzikas A, Shakir S, Gafoor S, Omran H, Nielsen-Kudsk JE, Kefer J, Aminian A, Berti S, Santoro G, Nietlispach F, Moschovitis A, Cruz-Gonzalez I, Stammen F, Tichelbäcker T, Freixa X, Ibrahim R, Schillinger W, Meier B, Sievert H, Gloekler S. Incidence and Clinical Impact of Device-Associated Thrombus and Peri-Device Leak Following Left Atrial Appendage Closure With the Amplatzer Cardiac Plug. *JACC Cardiovasc Interv*. 2017;10:391-9.
- Raphael CE, Friedman PA, Saw J, Pislaru SV, Munger TM, Holmes DR Jr. Residual leaks following percutaneous left atrial appendage occlusion: assessment and management implications. *EuroIntervention*. 2017;13:1218-25.
- Otton JM, Spina R, Sulas R, Subbiah RN, Jacobs N, Muller DW, Gunalingam B. Left Atrial Appendage Closure Guided by Personalized 3D-Printed Cardiac Reconstruction. *JACC Cardiovasc Interv*. 2015;8:1004-6.
- Hell MM, Achenbach S, Yoo IS, Franke J, Blachutzik F, Roether J, Graf V, Raaz-Schrauder D, Marwan M, Schlundt C. 3D printing for sizing left atrial appendage closure device: head-to-head comparison with computed tomography and transoesophageal echocardiography. *EuroIntervention*. 2017;13:1234-41.
- Goitein O, Fink N, Guetta V, Beinart R, Brodov Y, Konen E, Goitein D, Di Segni E, Grupper A, Glikson M. Printed MDCT 3D models for prediction of left atrial appendage (LAA) occluder device size: a feasibility study. *EuroIntervention*. 2017;13:e1076-9.

14. Nucifora G, Faletta FF, Regoli F, Pasotti E, Pedrazzini G, Moccetti T, Auricchio A. Evaluation of the left atrial appendage with real-time 3-dimensional transesophageal echocardiography: implications for catheter-based left atrial appendage closure. *Circ Cardiovasc Imaging*. 2011;4:514-23.
15. Saw J, Fahmy P, Spencer R, Prakash R, McLaughlin P, Nicolaou S, Tsang M. Comparing Measurements of CT Angiography, TEE, and Fluoroscopy of the Left Atrial Appendage for Percutaneous Closure. *J Cardiovasc Electrophysiol*. 2016;27:414-22.
16. Spencer R, DeJong P, Fahmy P, Lempereur M, Tsang M, Gin K, Lee PK, Nair P, Tsang TS, Jue J, Saw J. Changes in Left Atrial Appendage Dimensions Following Volume Loading During Percutaneous Left Atrial Appendage Closure. *JACC Cardiovasc Interv*. 2015;8:1935-41.
17. Roy AK, Horvilleur J, Cormier B, Cazalas M, Fernandez L, Patane M, Neylon A, Spaziano M, Sawaya FJ, Arai T, Bouvier E, Hovasse T, Lefèvre T, Chevalier B, Garot P. Novel integrated 3D multidetector computed tomography and fluoroscopy fusion for left atrial appendage occlusion procedures. *Catheter Cardiovasc Interv*. 2018;91:322-9.
18. Vukicevic M, Mosadegh B, Min JK, Little SH. Cardiac 3D Printing and its Future Directions. *JACC Cardiovasc Imaging*. 2017;10:171-84.
19. Binder TM, Moertl D, Mundigler G, Rehak G, Franke M, Delle-Karth G, Mohl W, Baumgartner H, Maurer G. Stereolithographic biomodeling to create tangible hard copies of cardiac structures from echocardiographic data: in vitro and in vivo validation. *J Am Coll Cardiol*. 2000;35:230-7.
20. Left Atrial Appendage Occlusion Guided by 3D Printing (LAA-PrintRegis). ClinicalTrials.gov Identifier: NCT03330210

Supplementary data

Supplementary Appendix. Methods.

Supplementary Figure 1. Summary of the 3D printing parameters used.

The supplementary data are published online at:
http://www.pcronline.com/eurointervention/135th_issue/29

